22nd International Conference
ENGINEERING MECHANICS 2016
Svratka, Czech Republic, 9 – 12 May 2016

PROBABILISTIC NONLINEAR ANALYSIS OF THE HERMETIC CIRCULAR COVER OF MAIN COOLANT PUMP FAILURE DUE TO EXTREME PRESSURE AND TEMPERATURE

J. Králik*

Abstract: *This paper describes the probabilistic nonlinear analysis of the hermetic circular cover of main coolant pump failure due to extreme pressure and temperature. The scenario of the hard accident in nuclear power plant (NPP) and the methodology of the calculation of the fragility curve of the failure overpressure using the probabilistic safety assessment PSA 2 level is presented. The model and resistance uncertainties were taken into account in the response surface method (RSM).*

Keywords: Nuclear Power Plant, Reactor cover, Nonlinearity, Fragility curve, PSA, RSM, ANSYS.

1. Introduction

After the accident of nuclear power plant (NPP) in Fukushimi the IAEA in Vienna adopted a large-scale project "Stress Tests of NPP", which defines a new requirements for the verification of the safety and reliability of NPP under extreme effects of internal and external environments and the technology accidents (Králik, 2009). The experience from these activities will be used to develop a methodology in the frame of the project ALLEGRO, which is focused to the experimental research reactor of 4th generation with a fast neutron core. This project is a regional (V4 Group) project of European interest. The new IAEA safety documents initiate the requirements to verify the hermetic structures of NPP loaded by two combinations of the extreme actions (Fig.1).

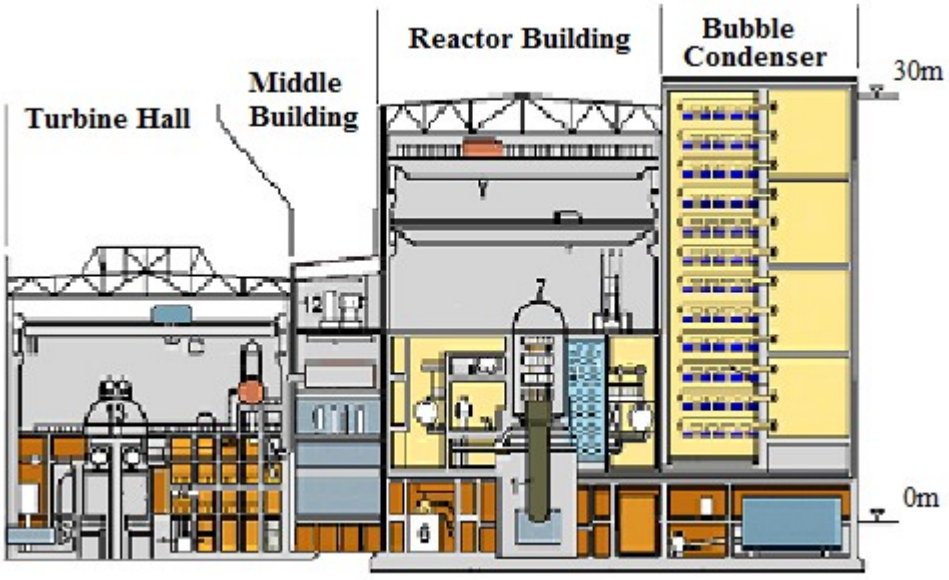

Fig 1: Section plane of the NPP with reactor VVER440/213

A first extreme load is considered for the probability of exceedance 10^{-4} by year and second for 10^{-2} by year. Other action effects are considered as the characteristic loads during the accident. In the case of the loss-of-coolant accident (LOCA) the steam pressure expand from the reactor hall to the bubble

* Prof.Ing.Juraj Králik,CSc.: Faculty of Civil Engineering, Slovak University of Technology Bratislava Radlinského 11; 810 05 Bratislava; SK, juraj.kralik@stuba.sk

condenser (Králik, 2010, 2015). The reactor and the bubble condenser reinforced structures with steel liner are the critical structures of the NPP hermetic zone (Králik, 2009). Next, one from the critical technology structures is the reactor hermetic cover. In the case of the hard accident the overpressure can be increased linearly and the internal and external temperature are constant. The critical technology steel segments are at level +18.9 (Fig.2). The safety and reliability of these segments were tested considering the scenario of the hard accidents.

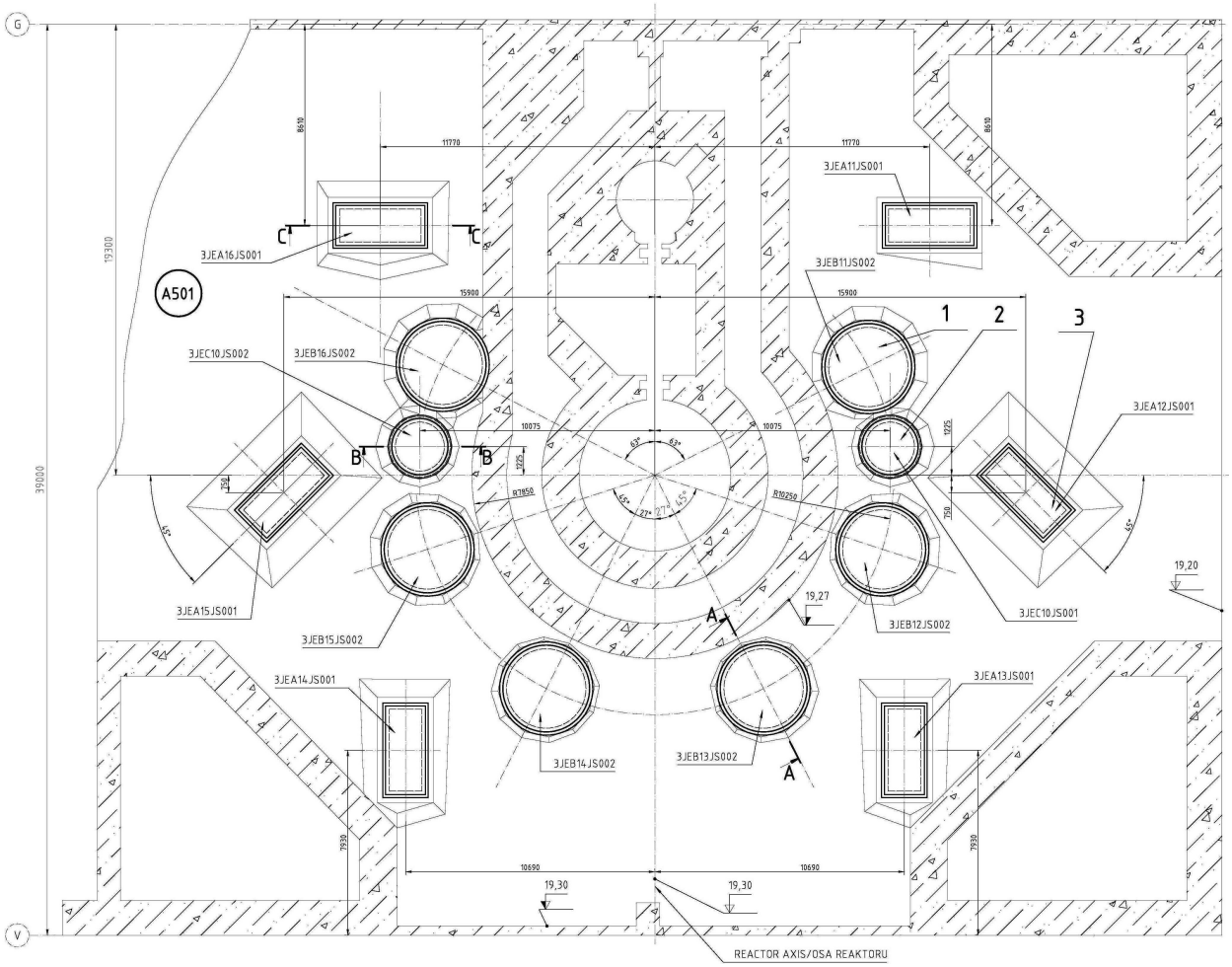

Fig 2: Situation of the hermetic cover at level +18,90m

2. Scenario of the accident

The previous analysis was achieved for the overpressure value of 100kPa due to design basic accident (DBA), which corresponds of the loss of coolant accident due to guillotine cutting of the coolant pipe (Králik, 2009). When the barbotage tower operates in the partial or zero performance the overpressure is equal to the 150 - 300 kPa.

Type	Duration	Overpressure in HZ [kPa]	Internal temperature [^oC]
I.	1hour - 1day	150	127
II.	2hours - 7days	250	150
III.	1year	-	80 - 120

Tab. 1: The assumed scenarios of the accidents in the hermetic zone

The ENEL propose the maximum temperature in the reactor shaft is equal about to 1 800^oC and in the containment around the reactor shaft is equal about to 350^oC (Králik, 2015). The possibility of the temperature increasing to the containment failure state is considered in the scenario too. In the case of the hard accident the overpressure can be increased linearly and the internal and external temperature are constant. Three types of the scenarios were considered (Tab.1). The critical was the accident during 7 days with the overpressure 250kPa, internal temperature 150^oC and external temperature -28^oC.

3. Calculation model

The steel coverings are located at the boundary of the confinement at floor level +18.90 m. In the assembled state, the steel covering fulfils both the sealing and shielding functions. The technology segments of the NPP hermetic zone are made from the steel. The MCP steel covering structure is shown in Fig. 3. The technical parameters of the covering basic parts are specified in Tab. 2. The shielding cover is fitted in the frame cast in concrete and sealed to the frame with double rubber packing of 15 mm in width. The shielding cover is provided with 30 mechanical closures along the circumference.

Part	Pos.	Basic dimension [mm]	Weight [kg]	Material
Welded frame	12	∅4000x500	1317	11373
Shielding cover	1	∅3710x160	13400	11378
Double protective cover	5	2x∅4000x30	2x632=1264	11373
Mechanical closures	9	30x235x180x150	420	422430/11700

Tab.2: Basic part of MCP Steel Covering

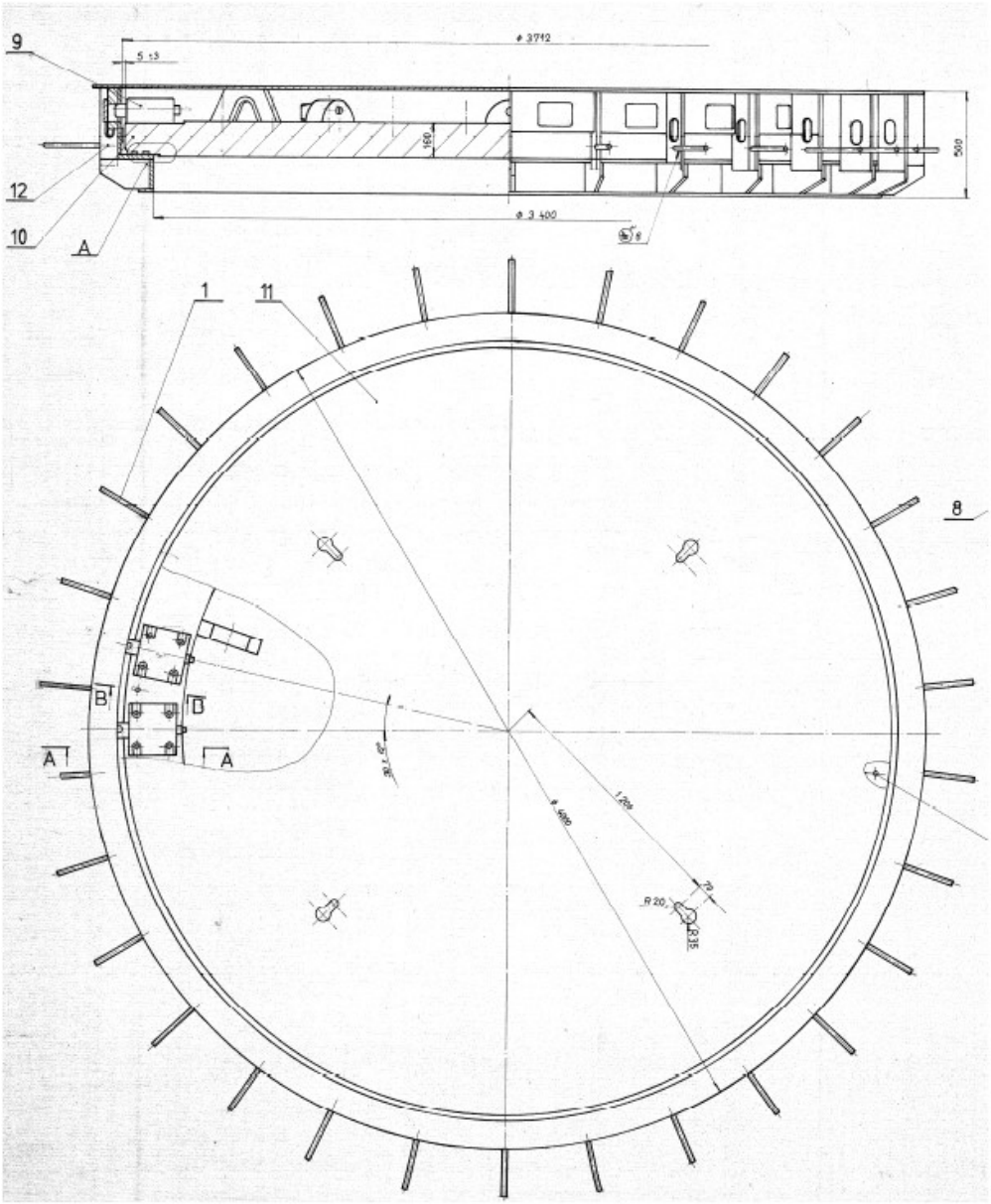

Fig.3: MCP Hermetic Steel Covering Structure

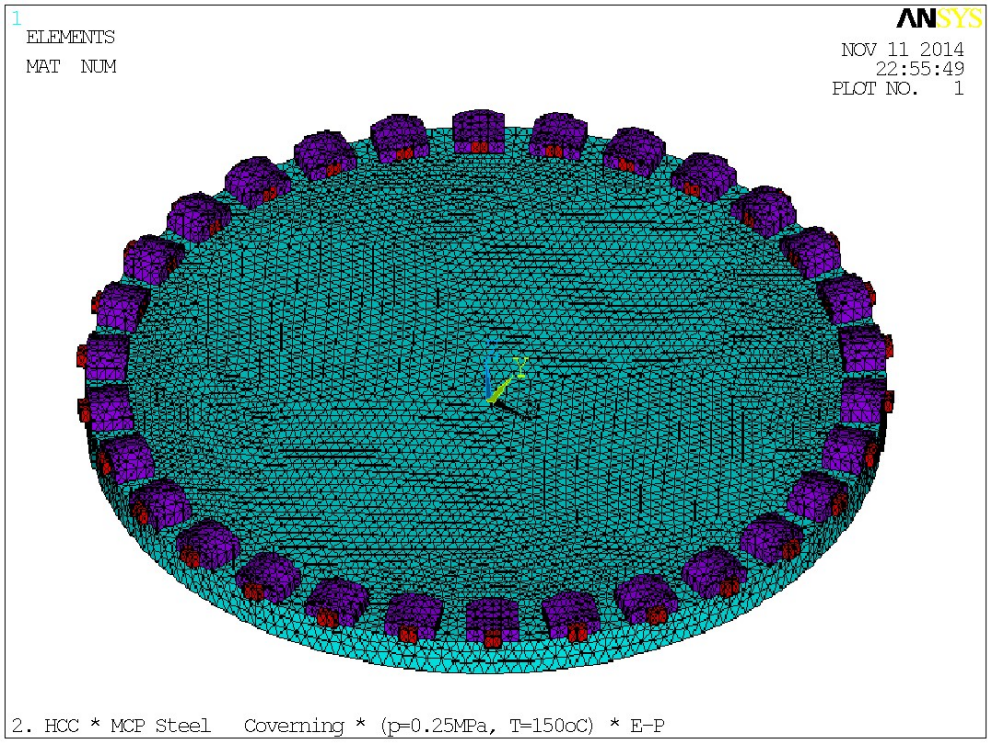

Fig.4: FEM model of the MCP Steel coverning

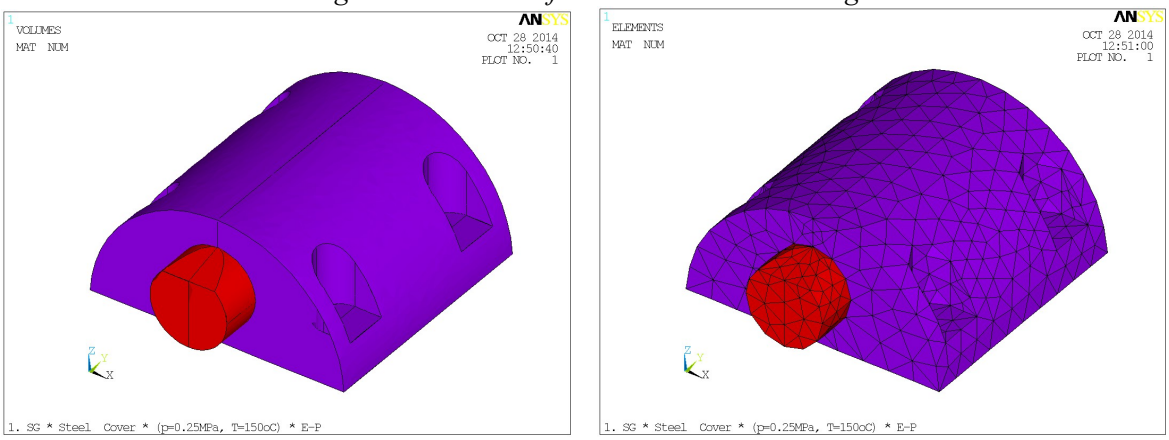

Fig.5: Solid and FEM model of the mechanical closure segment

Two calculation FEM models of the MCP steel covering structure with the mechanical closure were considered with two variants of the material properties of mechanical closure segments (Fig.4 and 5). The original closure segment is made from two materials - material 42 24 30 for mechanical closures, material 11700 for sliders. The FEM model has 107 212 solid and surface elements with 22 593 nodes.

4. Acceptance criteria

In the case of the nonlinear analysis the thermal depended material properties are used followind the input data for material 08CH18N10T defined in standard CSN 413240, CSN 411700, CSN 413230, CSN 413240 and NTD SAI Section II. The criterion for the max. stress values is limited by the H-M-H plastic potential (Králik, 2009). The failure of the steel structure is limited by the max. strain values or by the stability of the nonlinear solution (Kohnke, 2008).

The standard STN EN 1993 1-2 (Handbook, 2005) define following characteristic values of the strain for the structural steel :

- yield strain $\varepsilon_{ay,\theta} = 0,02$
- ultimate strain $\varepsilon_{au,\theta} = 0,15$

- max. limite strain $\varepsilon_{ae,\theta} = 0,20$

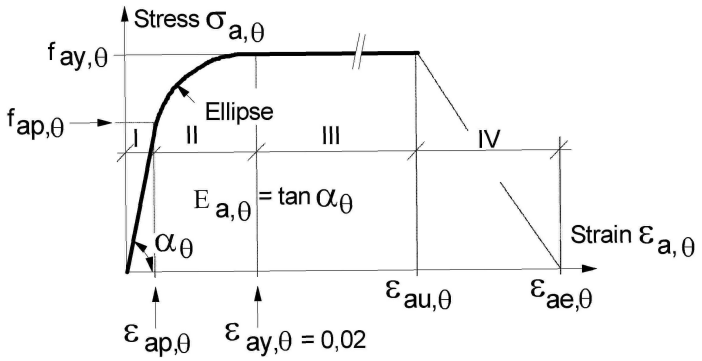

Fig.6: Stress-strain relationship of the steel dependent on temperature

The stress-strain relationship for the steel (Fig.6) are considered in accordance of Eurocode (Hanbook 5, 2005) on dependency of temperature level θ for heating rates between 2 and 50K/min. In the case of the steel the stress-strain diagram is divided on four regions.

The stress-strain relation $\sigma_{a,\theta} \approx \varepsilon_{a,\theta}$ are defined in following form in region I:

$$\sigma_{a,\theta} = E_{a,\theta}\varepsilon_{a,\theta}, \qquad E_{a,\theta} = k_{E,\theta}E_a \tag{1}$$

where the reduction factor $k_{E,\theta}$ can be chosen according to the values of (Hanbook 5, 2005).

In region II :

$$\sigma_{a,\theta} = \left(f_{ay} - c\right) + \frac{b}{a}\sqrt{a^2 - \left(\varepsilon_{ay,\theta} - \varepsilon_{a,\theta}\right)^2}\ , a^2 = \left(\varepsilon_{ay,\theta} - \varepsilon_{ap,\theta}\right)\left(\varepsilon_{ay,\theta} - \varepsilon_{ap,\theta} + c/E_{a,\theta}\right),$$

$$b^2 = E_{a,\theta}\left(\varepsilon_{ay,\theta} - \varepsilon_{ap,\theta}\right)c + c^2, \quad c = \frac{\left(f_{ay,\theta} - f_{ap,\theta}\right)^2}{E_{a,\theta}\left(\varepsilon_{ay,\theta} - \varepsilon_{ap,\theta}\right) - 2\left(f_{ay,\theta} - f_{ap,\theta}\right)} \tag{2}$$

and in region III :

$$\sigma_{a,\theta} = f_{ay,\theta} \tag{3}$$

5. Nonlinear analysis

The nonlinear analysis based on potential theory considering the isotropic material properties was made for the layered shell elements SHELL181 in the FEM model. The steel is typical isotropic material. The elastic-plastic behavior of the isotropic materials is described by the HMH yield criterion.

Consequently the stress-strain relations are obtained from the following relations

$$\{d\sigma\} = [D_{el}]\left(\{d\varepsilon\} - \{d\varepsilon^{pl}\}\right) = [D_{el}]\left(\{d\varepsilon\} - d\lambda\left\{\frac{\partial Q}{\partial \sigma}\right\}\right) \tag{4}$$

or

$$\{d\sigma\} = \left[D_{ep}\right]\{d\varepsilon\} \tag{5}$$

where $\left[D_{ep}\right]$ is elastic-plastic matrix in the form

$$\left[D_{ep}\right] = [D_e] - \frac{[D_e]\left\{\frac{\partial Q}{\partial \sigma}\right\}\left\{\frac{\partial F}{\partial \sigma}\right\}^T [D_e]}{A + \left\{\frac{\partial F}{\partial \sigma}\right\}^T [D_e]\left\{\frac{\partial Q}{\partial \sigma}\right\}} \tag{6}$$

The hardening parameter A depends on the yield function and model of hardening (isotropic or kinematic). Huber-Mises-Hencky (HMH) define the yield function in the form

$$\sigma_{eq} = \sigma_T(\kappa), \tag{7}$$

where σ_{eq} is equivalent stress in the point and $\sigma_o(\kappa)$ is yield stress depends on the hardening.
In the case of kinematic hardening by Prager (versus Ziegler) and the ideal Bauschinger's effect is given

$$A = \frac{2}{9E}\sigma_T^2 H' \tag{8}$$

The hardening modulus H' for this material is defined in the form

$$H' = \frac{d\sigma_{eq}}{d\varepsilon_{eq}^p} = \frac{d\sigma_T}{d\varepsilon_{eq}^p} \tag{9}$$

When this criterion is used with the isotropic hardening option, the yield function is given by:

$$F(\sigma) = \sqrt{\{\sigma\}^T [M]\{\sigma\}} - \sigma_o(\varepsilon_{ep}) = 0 \tag{10}$$

where $\sigma_o(\varepsilon_{ep})$ is the reference yield stress, ε_{ep} is the equivalent plastic strain and the matrix [M] is as follows

$$[M] = \begin{bmatrix} 1 & 0 & 0 & 0 & 0 & 0 \\ 0 & 1 & 0 & 0 & 0 & 0 \\ 0 & 0 & 1 & 0 & 0 & 0 \\ 0 & 0 & 0 & 2 & 0 & 0 \\ 0 & 0 & 0 & 0 & 2 & 0 \\ 0 & 0 & 0 & 0 & 0 & 2 \end{bmatrix} \tag{11}$$

On the base of the elastic-plastic theory and the HMH function of plasticity the extreme strain and stress of the reactor cover for the accident scenario type II are presented in the Tab. 3

Node	ε_1	ε_2	ε_3	ε_{int}	ε_{eqv}
Minimum Values of Strain					
Node	5206	5347	911	4707	3292
Value	-0.18645E-04	-0.10993E-03	-0.63748E-03	0.89030E-05	0.14470E-04
Maximum Values of Strain					
Node	1089	5316	22272	911	1948
Value	0.53063E-03	0.11104E-03	-0.15937E-05	0.95872E-03	0.70191E-03
Node	σ_1	σ_2	σ_3	σ_{int}	σ_{eqv}
Minimum Values of Stress [MPa]					
Node	5206	5347	911	4707	4707
Value	-14.065	-29.522	-129.51	1.0100	0.91042
Maximum Values of Stress [MPa]					
Node	1089	19589	106	911	911
Value	93.757	30.189	10.394	156.56	138.47

Tab.3: Extreme stress-strain values of the reactor protective hood for the accident scenario type II

6. Probability nonlinear assessment

The probabilistic methods are very effective to analyse of the safety and reliability of the structures considering the uncertainties of the input data (Čajka, R. Krejsa,M. ,2013, Gottwald, J. Kala, Z. , 2012, Haldar, A. Mahadevan, S., 2000, Kala, Z. ,2011, Konečný, P. Brožovsky, J. Krivý, V. ,2009, Králik,J. ,2009, 2010, Králik,J. et al. ,2015, Krejsa, M. Králik,J. ,2015, Melcher, J. et al. 2004, Novák, D. Bergmeister, K. Pukl, R. Červenka, V., 2009, Suchardová, P., et al. 2012, Sýkora,M. Holický,M. ,2013, Vejvoda, S., Keršner, Z., Novák, D. Teplý, B. ,2003). The probability analysis of the loss of the reactor cover integrity was made for the overpressure loads from 250 kPa to 1000 kPa using the nonlinear solution of the static equilibrium considering the geometric and material nonlinearities of the steel shell and beam elements. The probability nonlinear analysis of the technology segments is based on the proposition that the relation between the input and output data can be approximated by the approximation function in the form of the polynomial (Králik,J. ,2009). The full probabilistic assessment was used to get the probability of technology segment failure.

The safety of the technology segments was determined by the safety function *SF* in the form (Haldar, A. Mahadevan, S., 2000)

$$SF = E/R \qquad \text{and} \qquad 0 \le SF < 1 \tag{12}$$

where *E* is the action function and *R* is the resistance function.

The reliability function *RF* is defined in the form

$$RF = g(R,E) = 1 - SF = R - E > 0 \tag{13}$$

where $g(R,E)$ is the reliability function.

The probability of failure can be defined by the simple expression

$$P_f = P[R < E] = P[(R - E) < 0] \tag{14}$$

The reliability function *RF* can be expressed generally as a function of the stochastic parameters X_1, X_2 to X_n, used in the calculation of *R* and *E*.

$$RF = g(X_1, X_2, ..., X_n) \tag{15}$$

The failure function *g({X})* represents the condition (capacity margin) of the reliability, which can be either an explicit or implicit function of the stochastic parameters and can be single (defined on one cross-section) or complex (defined on several cross-sections, e.g., on a complex finite element model).

In the case of the nonlinear analysis the correct solution of the elastic-plastic behaviour of the structures is determined by the function plasticity. The HMH function of the plasticity was used for the nonlinear solution of the steel technology segments. This plasticity function is defined in the form

$$R = f_y \quad \text{and} \quad E = \sigma_{ef}, \tag{16}$$

where the effective stress σ_{ef} (Von Mises stress) is defined as follows

$$\sigma_{ef} = \left(\frac{1}{2} \left[(\sigma_1 - \sigma_2)^2 + (\sigma_2 - \sigma_1)^2 + (\sigma_3 - \sigma_1)^2 \right] \right)^{\frac{1}{2}}, \tag{17}$$

The failure of the steel technology segments in the frame of the PSA analysis is defined by the ultilimite values of the maximal strain deformation. This failure function is defined in the form

$$R = \varepsilon_{a\,y,\theta} \quad \text{and} \quad E = \varepsilon_{ef}, \tag{18}$$

where the effective strain ε_{ef} (Von Mises strain) is defined as follows

$$\varepsilon_{ef} = \frac{1}{1+\nu'} \left(\frac{1}{2} \left[(\varepsilon_1 - \varepsilon_2)^2 + (\varepsilon_2 - \varepsilon_1)^2 + (\varepsilon_3 - \varepsilon_1)^2 \right] \right)^{\frac{1}{2}}, \tag{19}$$

where ν' s the effective poisson constant.

The failure probability is calculated from the evaluation of the statistical parameters and theoretical model of the probability distribution of the reliability function $Z = g(X)$ using the simulation methods. The failure probability is defined as the best estimation on the base of numerical simulations in the form

$$p_f = \frac{1}{N}\sum_{i=1}^{N} I\left[g\left(X_i\right) \le 0\right] \tag{20}$$

where N in the number of simulations, $g(.)$ is the failure function, $I[.]$ is the function with value 1, if the condition in the square bracket is fulfilled, otherwise is equal 0.

The full probabilistic method result from the nonlinear analysis of the series simulated cases considered the uncertainties of the input data. The various simulation methods (direct, modified or approximation methods) can be used for the consideration of the influences of the uncertainty of the input data (Králik,J. ,2009).

In case of the nonlinear analysis of the full FEM model the approximation method RSM (Response surface method) is the most effective method (Králik,J. ,2009). The RSM is a method for constructing global approximations to system behaviour based on results calculated at various points in the design space (Fig.7). This method is based on the assumption that it is possible to define the dependency between the variable input and the output data through the approximation functions in the following form:

$$Y = c_o + \sum_{i=1}^{N} c_i X_i + \sum_{i=1}^{N} c_{ii} X_i^2 + \sum_{i=1}^{N-1}\sum_{j>i}^{N} c_{ij} X_i X_j \tag{21}$$

where c_o is the index of the constant member; c_i are the indices of the linear member and c_{ij} the indices of the quadratic member, which are given for predetermined schemes for the optimal distribution of the variables or for using the regression analysis after calculating the response. Approximate polynomial coefficients are given from the condition of the error minimum, usually by the "Central Composite Design Sampling" (CCD) method or the "Box-Behnken Matrix Sampling" (BBM) method (Králik,J. ,2009). The philosophy of the RSM method is presented in Fig.5. The original system of the global surface is discretized using approximation function. The design of the experiment determines the polynomic coefficients.

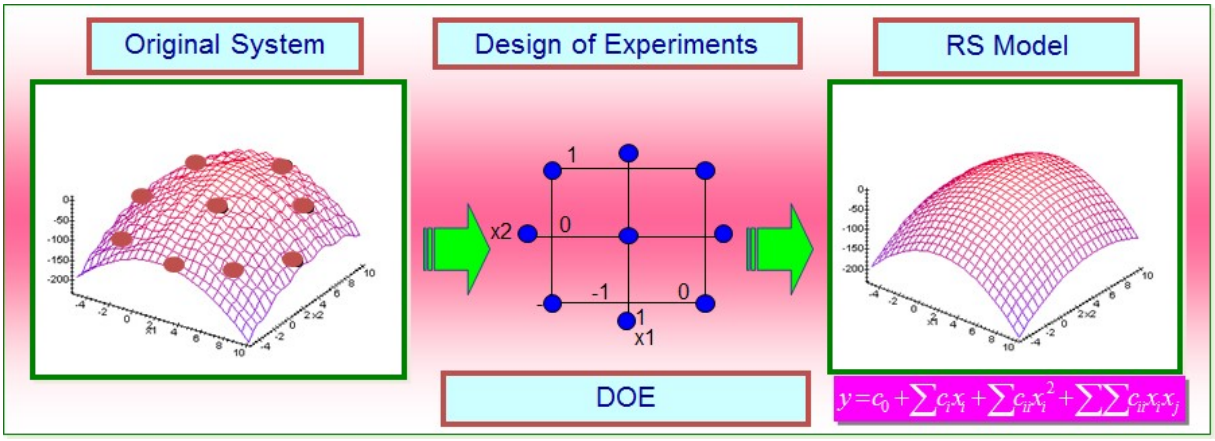

Fig.7: Scheme of the RSM approximation method with the CCD design experiment

The computation efficiency of the experimental design depends on the number of design points, which must be at least equal to the number of the unknown coefficients. In the classical design approach, a regression analysis is carried out to formulate the response surface after calculating the responses at the sampling points. These points should have at least 3 levels for each variable to fit the second-order polynomial, leading to 3k factorial design. This design approach becomes inefficient with the increasing of the number of random variables. More efficient is the central composite design, which was developed by Box and Wilson (Králik,J. ,2009).

The central CCD method is composed of (Fig. 7):

1. Factorial portion of design - a complete 2k factorial design (equal -1, +1)
2. Centre point - no centre points, no ≥ 1 (generally no =1)
3. Axial portion of design - two points on the axis of each design variable at distance α from the design centre

Then the total number of design points is $N = 2^k + 2k + n_o$, which is much more than the number of the coefficients p = (k+1) (k+2)/2.

The true performance function $g(\{X\})$ or $\{Y\}$ in Equation (21) can be represented in the matrix form as

$$\{Y\} = [X]\{c\} + \{\varepsilon\} \tag{22}$$

where $\{Y\}$ is the vector of actual responses, and [X] is the matrix of the combination coefficients.

The least squares estimates $\{\hat{c}\}$, defined as c_o, c_i, c_{ii} and c_{ij} in Equation (21), are obtained by solution of the least square (regression) analysis, i.e.

$$\{\hat{c}\} = \left([X]^T [X]\right)^{-1} [X]^T \{Y\} \tag{23}$$

The design includes several statistical properties such as orthogonality that makes the calculation of $[X]^T[X]$ term simple and rotability that insures the uniform precision of the predicted value.

The statistical postprocessor compiles the results numerically and graphically in the form of histograms and cumulative distributional functions. The sensibility postprocessor processes the data numerically and graphically and provides information about the sensitivity of the variables and about the correlation matrices.

On base of experimental design, the unknown coefficients are determined due to the random variables selected within the experimental region. The uncertainty in the random variables can be defined in the model by varying in the arbitrary amount producing the whole experimental region.

The total vector of the deformation parameters $\{r_s\}$ in the FEM is defined for the s^{th}-simulation in the form

$$\{r_s\} = \left[K_{GN}(E_s, F_\sigma)\right]^{-1} \{F(G_s, Q_s, P_s, T_s)\} \tag{24}$$

and the strain vector

$$\{\varepsilon_s\} = [B_s]\{r_s\} \tag{25}$$

where $[K_{GN}]$ is the nonlinear stiffness matrix depending on the variable parameters E_s and F_σ, F_σ is the Von Mises yield function defined in the stress components, $\{F\}$ is the vector of the general forces depending on the variable parameters G_s, Q_s, P_s and T_s for the s^{th}-simulation.

7. Uncertainties of the input data

The uncertainties are coming from the following sources (HANBOOK 5, 2005, JCSS, 2011, Králik,J. 2009, NRC, RG 1.200, 2009) :

- Parameters of material properties. Based on experiments with concrete elements the standard deviation is 11.1%. In case of other materials this value is about 5%.
- Assessment of mechanical characteristics error factors are about 8-12%, it depends on the construction material differences used for the different units with VVER 440/213. In some cases it can be conservative, in other cases non-conservative impact.
- Uncertainties in the numerical results in the value of 10-15%. In this area we can take into consideration the steel liner with the concrete elements.
- Uncertainties arising from the temperatures impact in the value of 10%.
- Other calculations assumptions 3-5%.

Quantity	Charact. value	Variable	Histog. type	Mean μ	Deviat. σ[%]	Minim. value	Maxim. value
Material							
Strength	F_k	f_{var}	N	1.1	6.6	0.774	1.346
Action effects							
Dead load	G_k	g_{var}	N	1	5	0.808	1.195
Live load	Q_k	q_{var}	GU	0.643	22.6	0.232	1.358

Pressure LOCA	p_k	p_{var}	N	1	8	0.698	1.333
Temperature	T_k	t_{var}	GU	0.667	14.2	0.402	1.147
Model uncertainties							
Action	E_k	e_{var}	N	1	5	0.813	1.190
Resistance	R_k	r_{var}	N	1	5	0.812	1.201

Tab. 4: Variability of input parameters

The mean values and standard deviations were defined in accordance of the experimental test and design values of the material properties and the action effects (see Tab.4). Based on the results from the simulated nonlinear analysis of the technology segments and the variability of the input parameters 10^6 Monte Carlo simulations were performed in the system ANSYS (Kohnke, P. 2008).

8. Probability and sensitivity nonlinear analysis of the reactor cover

The calculation of the probability of the reactor cover failure is based on the results of the nonlinear analysis for various level of the accident pressure and mean values of the material properties. The critical area of the technology segments defined from the nonlinear deterministic analysis is the mechanical closures. The CCD method of the RSM approximation is based on 45 nonlinear simulations depending on the 6 variable input data. The nonlinear solution for the one simulation consists about the 50 to 150 iteration depending on the scope of the plastic deformations in the calculated structures. The sensitivity analyses give us the informations about the influences of the variable properties of the input data to the output data (Fig.8 and 9). These analyses are based on the correlations matrixes.

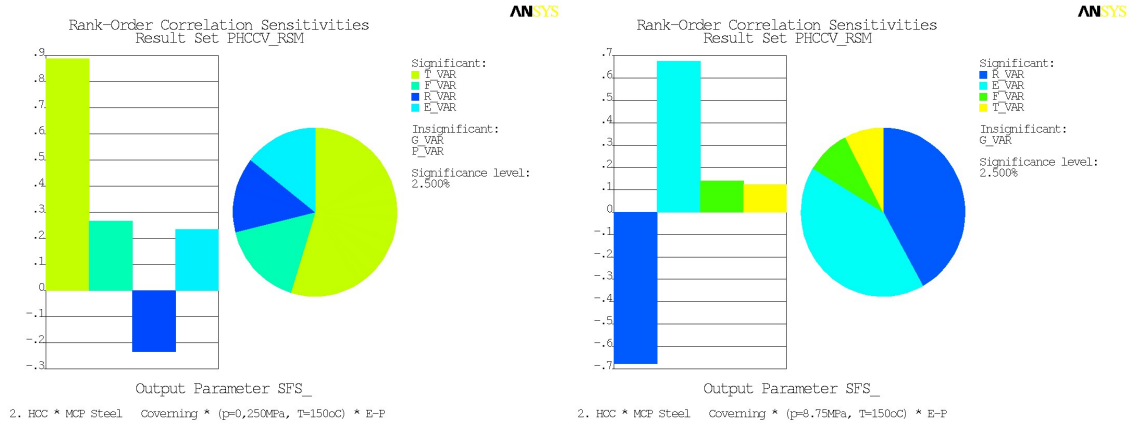

Fig.8: Sensitivity analysis of the safety function of MCP steel covering for overpressure Δp=0.25MPa and Δp=8.750MPa

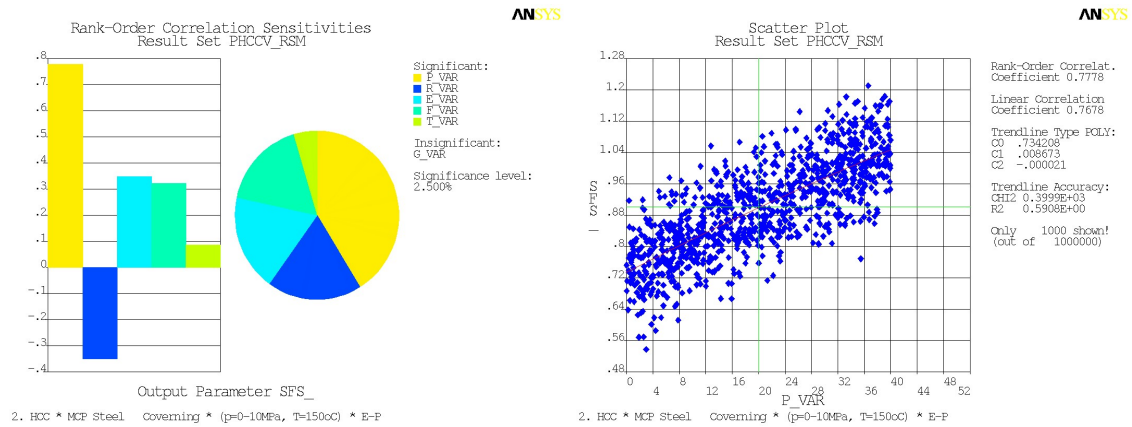

Fig.9: Sensitivity and trend analysis of the safety function of MCP steel covering for uniform distribution of overpressure

9. Fragility curves of failure pressure

The PSA approach to the evaluation of probabilistic pressure capacity involves limit state analyses (IAEA, 2010 and Králik, J. 2009). The limit states should represent possible failure modes of the confinement functions. Containment may fail at different locations under different failure modes. Consider two failure modes A and B, each with n fragility curves and respective probabilities p_i (i = 1,…,n) and q_j (j = 1,…,n). Then the union $C=A\cup B$, the fragility $F_{Cij}(x)$ is given by

$$F_{Cij}(x) = F_{Ai}(x) + F_{Bj}(x) - F_{Ai}(x) \cap F_{Bj}(x) \tag{26}$$

where the subscripts i and j indicate one of the n fragility curves for the failure modes and x denote a specific value of the pressure within the containment. The probability p_{ij} associated with fragility curve $F_{Cij}(x)$ is given by $p_i.\ q_j$ if the median capacities of the failure modes are independent. The result of the intersection term in (32) is $F_{Aj}(x)\ .F_{Bj}(x)$ when the randomness in the failure mode capacities is independent and $\min[F_{Ai}(x), F_{Bj}(x)]$ when the failure modes are perfectly dependent.

The following is and the consequence of an accident depends on the total leak area. Multiple leaks at different locations of the containment (e.g. bellows, hatch, and airlock) may contribute to the total leak area. Using the methodology described above, we can obtain the fragility curves for leak at each location.

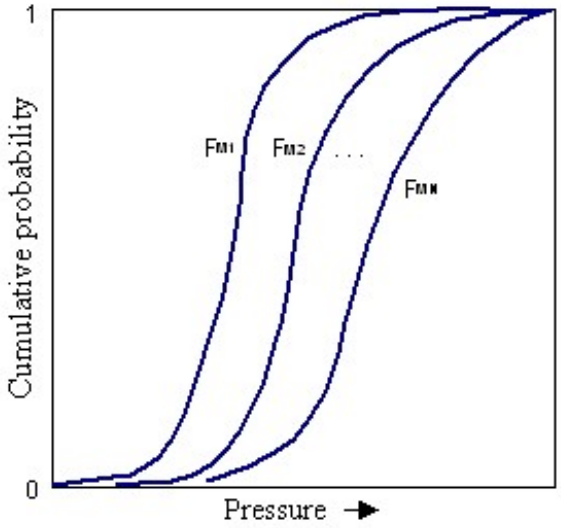

Fig. 10: Family of fragility curves showing modelling uncertainty

For a given accident sequence, the induced accident pressure probability distribution, $h(x)$, is known. This is convolved with the fragility curve for each leak location to obtain the probability of leak from that location (P_{Li}). It is understood that there is no break or containment rupture at this pressure.

$$p_{Li} = \int_0^\infty h(x)\left[1 - F_b(x)\right] F_l(x)\,dx\,, \tag{27}$$

here $F_b(x)$ is the fragility of break at the location and $F_l(x)$ is the fragility of leak. The leak is for each location specified as a random variable with a probability distribution.

The probability of reactor cover failure is calculated from the probability of the reliability function RF in the form,

$$P_f = P(RF < 0) \tag{28}$$

where the reliability condition RF is defined depending on a concrete failure condition

$$RF = 1 - \varepsilon_{ef} \,/\, \varepsilon_{a\,y,\theta}\,, \tag{29}$$

where the failure function was considered in the form (18).

The fragility curve of the failure pressure was determined using 45 probabilistic simulations using the RSM approximation method with the experimental design CCD for 10^6 Monte Carlo simulations for each model and 5 level of the overpressure. The various probabilistic calculations for 5 constant level of overpressure next for the variable overpressure for gauss and uniform

distribution were taken out. The failure criterion of the steel structures using HMH (Von Mises) plastic criterion with the multilinear kinematic hardening stress-strain relations for the various level of the temperatures and the degradation of the strength were considered. The uncertainty of the input data (Tab. 4) and the results of the nonlinear analysis of the technological structures for various level of the accident pressure were taken. The overpressure loads from 250kPa to 10 000kPa using the nonlinear solution of the static equilibrium considering the geometric and material nonlinearities of the steel solid and shell layered elements were considered. The recapitulation of the probability of failure calculated by the RSM simulation method is presented in Fig. 11 depending on the level of the pressure.

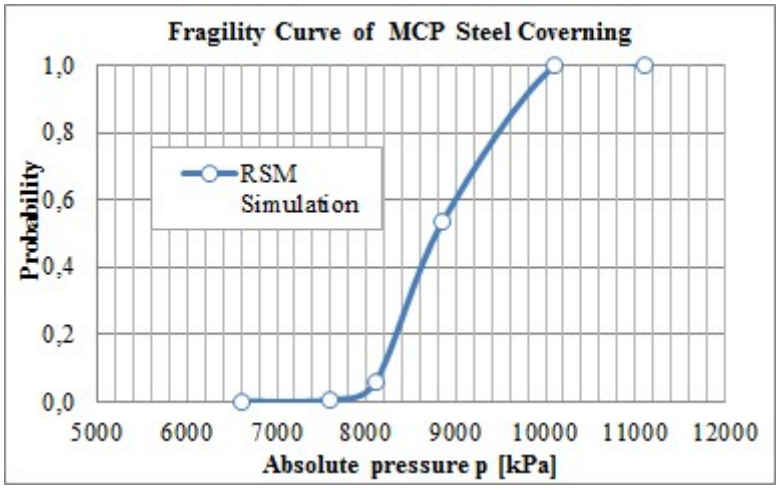

Fig.11: Fragility curve of MCP steel covering determined by approximation method a RSM with CCD experimental design

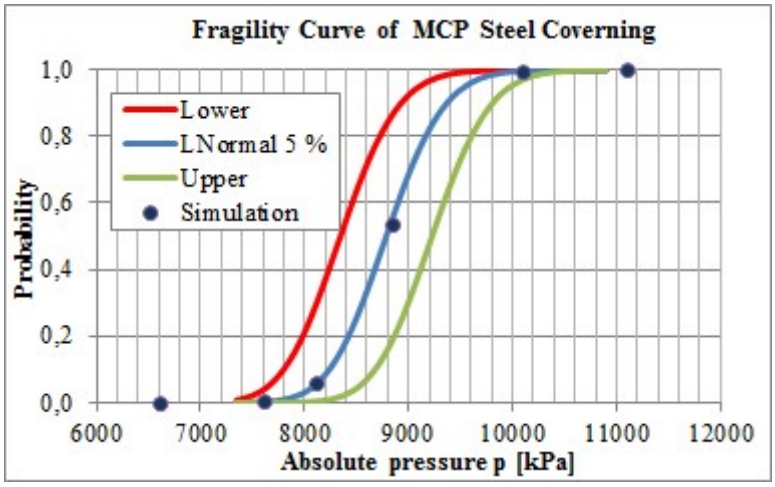

Fig.12: Fragility curves of MCP steel covering determined analytically for normal distribution with 5% envelope

10. Conclusions

This report is based on methodology of the probabilistic analysis of structures of hermetic zone of NPP with reactor VVER44/213 detailed described in work (Králik,J. 2009). The nonlinear probabilistic analysis of MCP steel covering failure is in accordance with the requirements (IAEA, 2010) and NRC (NRC, RG 1.200, 2009, NUREG/CR-6906, 2006), experiences from the similar analysis NPP in abroad (Novák, at al. 2009), new knowledges from the probabilistic analysis of structures (Čajka, R. Krejsa,M. 2013, Haldar, A.Mahadevan, S., 2000, IAEA,2010, JCSS,2011, Kala, Z. 2011). Sensitivity analysis of steel plane frames with initial imperfections (Kala, Z. 2011) and our experiences from the previous analysis (Krejsa, M. 2014, Krejsa, M. Králik,J. 2015, Králik,J. 2009, 2010 and 2015).

These analyses go out from the previous results of the monitoring of material properties and NPP structures, as well as from the results of the resistance analysis of the important structural components

from the point of the initiated accidents. The structures were analysed on impact of the extreme loads situation defined in the scenarios of the internal accidents.

According to the nonlinear deterministic analysis were defined the most critical structural components for which the values of the failure pressure of the accident are determined on base of the best estimation. We propose from the supposition that the loss of containment integrity occur and the performance of the NPP can be unsafe. The critical elements were identified taking into consideration also uncertainties of the input data in the results.

The nonlinear analysis of the loss of the containment integrity was made for the overpressure loads from 250kPa using the nonlinear solution of the static equilibrium considering the geometric and material nonlinearities of the steel shell and solid elements. The nonlinear analyses were performed in the ANSYS program using the HMH plastic condition (Kohnke, P. 2008).

The standard STN EN 1993 1-2 (HANBOOK 5. 2005) define following characteristic values of the strain for the structural steel - yield strain and ultimate strain. The recapitulation of the capacity check based on deterministic analysis is presented in Tab. 3.

The probability analysis of the loss of the concrete containment integrity was made for the overpressure loads from 250kPa to 10 000kPa using the nonlinear solution of the static equilibrium. The uncertainties of the loads level (temperature, dead and live loads), the material model of the steel structures as well as the inaccuracy of the calculation model and the numerical methods (Králik,J. 2009) were taken into account in the approximation RSM method for CCD experimental design and 10^6 Monte Carlo simulations.

One from the critical technology segments of the containment is MCP steel covering with the failure pressure $p_{u.0,05}$=8023.7kPa. The mean value of pressure capacity of MCP steel covering is $p_{u.0,50}$=8795.5kPa, the upper bound of 95% is $p_{u.0,95}$=9971.7kPa. These fragility curves (Fig.12) are the input data for the following risk analysis of the NPP safety.

Acknowledgements

The project was performed with the financial support of the Grant Agency of the Slovak Republic (VEGA 1/0265/16).

References

Abraham, (1998) ASME Boiler and Pressure Vessel Code, Section III, Div. 1, Appendix F, "*Rules for Evaluation of Service Loadings with Level D Service Limits*," American Society of Mechanical Engineers.

Čajka, R. Krejsa,M. (2013) Measured Data Processing in Civil Structure Using the DOProC, Method, *Advanced Materials Research* Vol. 859, p. 114-121, DOI 10.4028/www.scientific.net/ AMR.859.114, December.

ENSREG, (2012) *Post-Fukushima accident. Action Plan. Follow-up of the peer review of the stress tests performed on European nuclear power plants*.

Gottwald, J. and Kala, Z. (2012) Sensitivity analysis of tangential digging forces of the bucket wheel excavator SchRs 1320 for different terraces. *Journal of Civil Engineering and Management*, 18:5, 609-620.

Haldar, A. and Mahadevan, S., (2000) Probability, Reliability and Statistical Methods in Engineering Design, John Wiley & Sons, New York.

HANBOOK 5. (2005) *Implementation of Eurocodes Reliability Backgrounds. Design of Buildings for the Fire Situation. Development of Skills Facilitating Implementatio of Eurocodes*. Leonardo Da Vinci Pilot Project CZ/02/B/F/PP-134007. Prague, CR.

IAEA (2010) *Safety Series No. SSG-4, Development and Application of Level 2 Proba-bilistic Safety Assessment for Nuclear Power Plants*, Vienna.

JCSS 2011. *JCSS Probabilistic Model Code.* Zurich: Joint Committee on Structural Safety. <www.jcss.byg.dtu.dk>.

Kala, Z. (2011) Sensitivity analysis of steel plane frames with initial imperfections, *Engineering Structures*, 33, 8, pp.2342-2349.

Kohnke, P. (2008) *ANSYS, Theory,* SAS IP Inc. Canonsburg.

Konecny, P. Brozovsky, J. Krivy, V. (2009) Simulation Based Reliability Assessment Method using Parallel Computing. In *Proceedings of 1st International Conference on Parallel, Distributed and Grid Computing for Engineering, Civil Comp Proceedings*, issue 90, pp. 542–549 (8 p), ISSN: 1759-3433

Králik,J. (2009) *Safety and Reliability of Nuclear Power Buildings in Slovakia. Earthquake-Impact-Explosion.* Ed. STU Bratislava, 307pp. ISBN 978-80-227-3112-6.

Králik,J. (2009) *Reliability Analysis of Structures Using Stochastic Finite Element Method*, Ed. STU Bratislava, 143pp. ISBN 978-80-227-3130-0.

Králik,J. (2010) Probabilistic Safety Analysis of the Nuclear Power Plants in Slovakia. In: *Journal of KONBiN*, Safety and Reliability Systems, Ed. VERSITA Central European Science Publishers, Warszawa, ISSN 1895-8281, No 2,3 (14, 15) pp. 35-48.

Králik,J. et al. (2015) Structural Reliability for Containment of VVER 440/213 Type, In *Safety and Reliability: Methodology and Applications - Nowakowski et al.* (Eds) © Taylor & Francis Group, London, p.2279-2286.

Krejsa, M. (2014) Probabilistic failure analysis of steel structures exposed to fatigue, In. *Key Engineering Materials*, Vol. 577-578, Pp. 101-104.

Krejsa, M. Králik,J. (2015) Probabilistic Computational Methods in Structural Failure Analysis, Journal of Multiscale Modelling, Vol. 6, No. 2 (5 pages), Imperial College Press, DOI: 10.1142/S1756973715500067.

Melcher, J., Kala, Z., Holický, M., Fajkus, M. & Rozlívka, L. (2004) Design characteristics of structural steels based on statistical analysis of metallurgical products. Journal of Constructional Steel Research, 60, 3-5, pp.795-808.

Novák, D. Bergmeister, K. Pukl, R. Červenka, V., (2009) Structural assessment and reliability analysis for existing engineering structures, Theoretical background. *Structure and infrastructure engineering*, Vol. 9, No. 2, pp. 267-275.

NRC, RG 1.200, (2009) *An Approach for Determining the Technical Adequacy of Probabilistic Risk Assessment Results for Risk-Informed Activities*, U.S. Nuclear Regulatory Commission, Washington, DC.

NUREG/CR-6906, (2006) *Containment Integrity Research at Sandia National Laboratories*, An Overview, Sandia National Laboratories, SAND2006-2274P, US NRC Washington, July.

Suchardová, P., Bernatík, A., Sucharda, O. (2012) Assessment of loss results by means of multi - Criteria analysis. In: Advances in Safety, Reliability and Risk Management, *Proc. of the European Safety and Reliability Conference, ESREL 2011*. London: CRC Press-Taylor & Francis group, pp. 1563-1570. ISBN 978-0-415-68379-1.

Sýkora,M. Holický,M. (2013) Assessment of Uncertainties in Mechanical Models, *Applied Mechanics and Materials*, Vol. 378 pp 13-18, © Trans Tech Publications, Switzerland, doi:10.4028/www.scientific.net/AMM.378.13.

Vejvoda, S., Keršner, Z., Novák, D. Teplý, B. (2003) Probabilistic Safety Assessment of the Steam Generator Cover, In *Proc. of the 17th International Conference on Structural Mechanics in Reactor Technology* (SMiRT 17), Prague, Czech Republic, August 17-22, in CD, M04-4, 10 pp.